Virus inactivation in the presence of quartz sand under static and dynamic batch conditions at different temperatures

2 AUTHORS:

Constantinos V. Chrysikopoulos
Technical University of Crete
143 PUBLICATIONS **2,004** CITATIONS

SEE PROFILE

Andriana Aravantinou
University of Patras
9 PUBLICATIONS **28** CITATIONS

SEE PROFILE

Virus inactivation in the presence of quartz sand under static and dynamic batch conditions at different temperatures
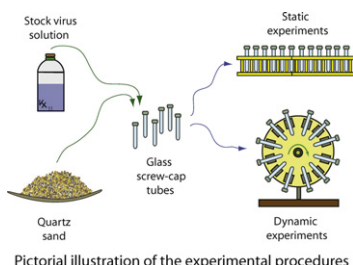
Constantinos V. Chrysikopoulos*, Andriana F. Aravantinou

Environmental Engineering Laboratory, Civil Engineering Department, University of Patras, Patras 26500, Greece

GRAPHICAL ABSTRACT

Pictorial illustration of the experimental procedures

ABSTRACT

Virus inactivation is one of the most important factors that controls virus fate and transport in the subsurface. In this study the inactivation of viruses in the presence of quartz sand was examined. The bacteriophages MS2 and ΦX174 were used as model viruses. Experiments were performed at 4 °C and 20 °C, under constant controlled conditions, to investigate the effect of virus type, temperature, sand size, and initial virus concentration on virus inactivation. The experimental virus inactivation data were satisfactorily represented by a pseudo-first order expression with time-dependent rate coefficients. Furthermore, the results indicated that virus inactivation was substantially affected by the ambient temperature and initial virus concentration. The inactivation rate of MS2 was shown to be greater than that of ΦX174. However, the greatest inactivation was observed for MS2 without the presence of sand, at 20 °C. Sand surfaces offered protection against inactivation especially under static conditions. However, no obvious relationship between sand particle size and virus inactivation could be established from the experimental data. Moreover, the inactivation rates were shown to increase with decreasing virus concentration.

© 2012 Elsevier B.V. All rights reserved.

1. Introduction

In many parts of the world, where surface water supplies are limited or polluted, groundwater is the single most important source of drinking water [1]. Microbial contamination of groundwater often leads in large outbreaks of waterborne diseases [2,3]. Consequently, in order to protect the public health, it is most important to fully understand the various factors controlling pathogen survival in the subsurface. Worthy to note is that viruses are the most disinfection-resistant microbial pathogens and exhibit quite conservative transport behavior in groundwater [4–7].

Pathogens in groundwater can originate from numerous accidental and intentional sources of pollution (e.g. landfills, broken sewer pipelines, leaking septic tanks, graveyards, urban runoff, irrigation, direct injection wells, and recharge basins) [8–10]. Furthermore, as the demand for clean water increases and supplies are depleted fast, artificial groundwater recharge has progressively increased to reverse the rapid depletion of aquifers [7,11,12]. Therefore, a major concern with using recycled water is that infective human enteric viruses might be delivered directly into the subsurface environment.

The fate and transport of viruses in porous and fractured subsurface formations is controlled by attachment onto mineral surfaces,

Nomenclature

C	aqueous phase concentration of viruses, M/L
C_0	initial aqueous phase concentration of viruses, M/L
C_u	coefficient of uniformity, –
d_{10}	sand grain diameter size that can barely pass through a sieve, which allows 10% of the material (by weight) to pass through, L
d_{60}	sand grain diameter size that can barely pass through a sieve, which allows 60% of the material (by weight) to pass through, L
I_s	ionic strength, mol/L
t	time, t
α	resistivity coefficient, $1/t$
λ	inactivation rate coefficient, $1/t$
λ_0	initial inactivation rate coefficient, $1/t$

Abbreviations

CQS	coarse quartz sand
ddH$_2$O	distilled deionized water
FQS	fine quartz sand
MQS	medium quartz sand
PBS	phosphate buffered saline
pfu	plaque forming units

inactivation (loss of infective capability), water chemistry, and temperature [13–25]. Numerous studies have been focused on virus attachment onto natural and model aquifer materials [26–36]. In contrast, although several experimental and theoretical studies have been conducted on virus inactivation [37–45], additional research is still needed in order to fully understand virus inactivation in complex subsurface formations.

The present study aims to investigate the inactivation of bacteriophages MS2 and ΦX174 in the presence of quartz sand materials with various particle sizes. A relatively large number of virus inactivation experiments were conducted under static and dynamic conditions. Furthermore, inactivation rate coefficients were determined by fitting a time-dependent inactivation model to the experimental data. To our knowledge the effect of initial virus concentration on virus inactivation is not fully understood. Furthermore, the combined effects of initial virus concentration, sand particle size, and temperature on inactivation of bacteriophages MS2 and ΦX174 have not been previously explored.

2. Experimental

2.1. Bacteriophages and quartz sand

The bacteriophages MS2 and ΦX174 were used in this study because they are similar to enteric viruses in size, shape, and surface characteristics [46]. MS2 is a F-specific, single-stranded RNA-phage (31% nucleic acid content) with host bacterium *Escherichia coli* ATTC 15597-B1, particle diameter 24–26 nm, and isoelectric point (pH$_{iep}$) of 4.1 [30]. ΦX174 is an icosahedral, single-stranded DNA-phage (26% nucleic acid content) with host bacterium *E. coli* ATTC 13706-B1, particle diameter 25–27 nm, and pH$_{iep}$ = 4.4 [30]. Furthermore, MS2 has a hydrophobic protein coat, whereas ΦX174 has a hydrophilic protein coat [47]. For the preparation of stock and purification of bacteriophages, the ATCC procedure [48] as outlined by Syngouna and Chrysikopoulos [49] was employed.

Three different size distributions of quartz sand (Filcom Filterzand & Grind) were used in the experiments: fine quartz sand (FQS) with grain diameter ranging from 0.150 to 0.212 mm (sieve no. 70/100), medium quartz sand (MQS) with grain diameter

ranging from 0.425 to 0.600 mm (sieve no. 30/40), and coarse quartz sand (CQS) with grain diameter ranging from 1.180 to 1.700 mm (sieve no. 12/16). Particle size distribution values obtained by sieve analysis were used to calculate the coefficient of uniformity, $C_u = d_{60}/d_{10}$ (were d_{10}, and d_{60} is the diameter of a sand grain that is barely too large to pass through a sieve that allows 10%, and 60%, respectively, of the material (by weight) to pass through). The coefficient of uniformity for each sand distribution was determined as: $C_u = 1.19, 1.21, 1.2$ for FQS, MQS, CQS, respectively. The chemical composition of the quartz sand as reported by the manufacturer (Filcom, Netherlands) was: 96.2% SiO$_2$, 0.15% Na$_2$O, 0.11% CaO, 0.02% MgO, 1.75% Al$_2$O$_3$, 0.78% K$_2$O, 0.06% SO$_3$, 0.46% Fe$_2$O$_3$, 0.03% P$_2$O$_5$, 0.02% BaO, 0.01% Mn$_3$O$_4$, and 0.28% loss on ignition. The three quartz sand distributions were thoroughly cleaned with 0.1 M nitric acid HNO$_3$ (70%) for 3 h to remove surface impurities (e.g. iron hydroxide and organic coatings) that could promote physicochemical deposition of the viruses, rinsed with distilled deionized water (ddH$_2$O), then soaked in 0.1 M NaOH for 3 h, and rinsed with ddH$_2$O again [5]. Subsequently, the sand distributions were sterilized and dried in an oven at 105 °C for 24 h.

2.2. Static and dynamic batch experiments

Batch experiments were conducted with MS2 and ΦX174 in the presence of three different quartz sand distributions (FQS, MQS, CQS) to examine the effect of quartz sand particle size on virus inactivation. The static batch experiments were performed under controlled conditions at 4 °C and 20 °C, and the dynamic experiments at 4 °C. Several virus stock solutions with concentrations ranging from 10^3 to 10^8 pfu/mL were used for both static and the dynamic experiments. At least 5 different virus stock concentrations were used for the static experiments, and 3 different virus stock concentrations were used for the dynamic experiments. Furthermore, thirty-nine experiments for each virus (MS2, ΦX174) were conducted under various conditions.

All batch experiments were performed in 20 mL Pyrex glass screw-cap tubes (Fisher Scientific). Glass tubes were washed with detergent, soaked in 6 N HCl, rinsed thoroughly in ddH$_2$O, autoclave sterilized, and oven dried at 105 °C overnight. A phosphate buffered saline (PBS) solution with low ionic strength (I_s) was prepared with 1.2 mM NaCl, 0.027 mM KCl, and 0.010 mM phosphate buffer salts in ddH$_2$O and adjusted to a pH 7.5 with HCl [45]. The specific conductance of the final virus suspension was 212 μS/cm, which corresponds to $I_s \approx 2$ mM. Note that the PBS solution was used to enhance virus stability by eliminating unspecified factors that could cause virus inactivation [50]. The stock solutions of bacteriophage MS2 and ΦX174, with concentrations in excess of 10^9 pfu/mL, were diluted with PBS solution to yield the desired bacteriophage concentration.

For each experiment, 30 glass tubes were employed, which were divided into two groups. Each group consisted of 15 glass tubes. The glass tubes of the first group (experimental tubes) contained 14 mL of virus suspension with 14 g of sand, and the glass tubes of the second group (control tubes) contained 14 mL of virus suspension without sand. All glass tubes were filled to the top. However, a small air bubble was always trapped within the tubes when the caps were screwed onto the tubes. Both groups were treated in the same manner. The static batch experiments were conducted in a constant-temperature dark room at 4 °C, and in an incubator at 20 °C. The dynamic batch experiments were performed in the constant-temperature dark room at 4 °C, with all the tubes attached to a tube rotator (Selecta, Agitador orbit), operated at 12 rpm, in order to allow the sand to mix within the virus solution. All the experiments were conducted in a dark room to eliminate the possibility of inactivation by sunlight [51]. One tube of each group was chosen at random at pre-determined time intervals during
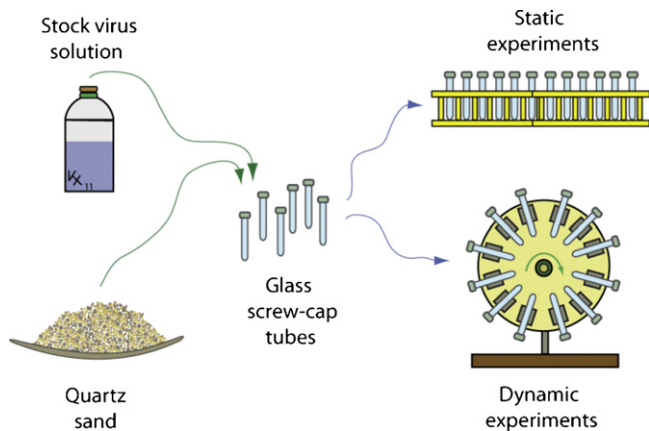
Stock virus
solution

Static
experiments

Glass
screw-cap
tubes

Quartz
sand

Dynamic
experiments

Fig. 1. Pictorial illustration of the experimental procedures. Glass screw-cap tubes received virus stock solution and quartz sand (control tubes received only the virus solution). Static batch experiments were conducted with all glass tubes placed in a rack; whereas, dynamic batch experiments were performed with all glass tubes attached to a tube rotator.

the experiment. Control tubes, in the absence of sand, were used to monitor virus inactivation caused by factors other than virus attachment onto the quartz sand. A sample of the PBS solution (1.0 mL) was removed from each selected glass tube at different preselected times (0, 1, 2, 3, 4, 5, 7, 14, 21, 30, 45, 60, and 75 days) and assayed for bacteriophage MS2 and ΦX174. Then, the used glass tubes were discarded. Fig. 1 presents an illustration of the batch experimental procedures employed in this work.

3. Theoretical considerations

The experimental data from numerous batch inactivation studies have been successfully described by a pseudo-first-order expression with a time-dependent rate coefficient as follows [42,44,45]:

$$\frac{dC(t)}{dt} = -\lambda(t)C(t) \tag{1}$$

where C is the concentration of suspended viruses in the liquid phase, t is time, and λ is the time-dependent inactivation rate coefficient of suspended viruses described by the following expression:

$$\lambda(t) = \lambda_0 e^{-\alpha t} \tag{2}$$

where λ_0 is the initial inactivation rate coefficient, and α is the resistivity coefficient. Assuming that $C(0) = C_0$, where C_0 is the initial virus concentration, the solution to Eq. (1) is:

$$\ln\left[\frac{C(t)}{C_0}\right] = -\frac{\lambda_0}{\alpha}\left\{\exp[-\alpha t] - 1\right\} \tag{3}$$

For the special case where $\lambda(t) = \lambda$ the solution to Eq. (1) is the following familiar expression:

$$\ln\left[\frac{C(t)}{C_0}\right] = -\lambda t \tag{4}$$

The unknown inactivation parameter values λ_0 and α were obtained by fitting Eq. (3) to the experimental log-normalized-concentration data using non-linear least squares algorithms, whereas the unknown parameter λ was estimated by linear regression fit of Eq. (4) to the log-normalized experimental data.

4. Results

The experimental data from the batch experiments of MS2 and ΦX174 inactivation at 4 °C are shown in Figs. 2 and 3, respectively. It should be noted that normalized bacteriophage concentrations over 1 are due to slight variations in the initial concentration of the virus suspensions present in each tube. The experimental data were fitted with both the time-dependent inactivation model and the time-invariant inactivation model. The parameters λ_0 and α were determined by fitting Eq. (3) to the observed normalized bacteriophage log-concentrations, whereas λ values were determined by linear regression fit to Eq. (4) of the same experimental data. The fitted virus inactivation parameter values (λ_0, α and λ) for MS2 are listed in Table 1, and for ΦX174 are listed in Table 2. Note that only simulated concentrations based on the time-dependent inactivation are shown in Figs. 2 and 3 because the time-dependent inactivation model matched the experimental inactivation data much better than the constant inactivation model. For all three quartz sand distributions considered in this study (FQS, MQS, and
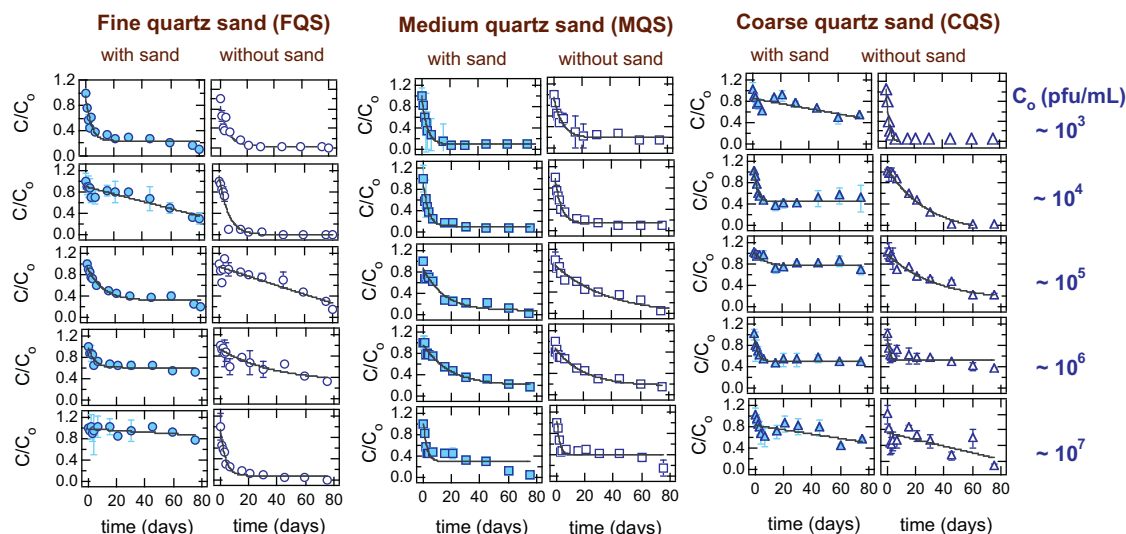
Fig. 2. Experimental data for MS2 inactivation under static batch conditions with sand (solid symbols) and without sand (open symbols) at 4 °C, and simulated concentration histories (solid curves). The first row of graphs corresponds to virus initial concentration of $C_0 = 10^3$ pfu/mL, the second, third, fourth and fifth rows to $C_0 = 10^4$, 10^5, 10^6, and 10^7 pfu/mL, respectively. The circles, squares, and triangles represent experiments with FQS, MQS, and CQS, respectively. Error bars not shown are smaller than the size of the symbol.

Table 1
Fitted inactivation parameters for bacteriophage MS2.

Conditions[a]		Static batch experiments at 4 °C				Static batch experiments at 20 °C				Dynamic batch experiments at 4 °C			
		C_0 (pfu/mL)	λ_0 (day^{-1})	α (day^{-1})	λ (day^{-1})	C_0 (pfu/mL)	λ_0 (day^{-1})	α (day^{-1})	λ (day^{-1})	C_0 (pfu/mL)	λ_0 (day^{-1})	α (day^{-1})	λ (day^{-1})
FQS	w	2.5×10^3	0.174 ± 0.016	0.030 ± 0.007	0.029 ± 0.003	2.1×10^3	0.036 ± 0.002	0.004 ± 0.002	0.029 ± 0.001	5.3×10^4	0.051 ± 0.016	0.007 ± 0.007	0.023 ± 0.001
	w/o		0.245 ± 0.041	0.021 ± 0.009	0.068 ± 0.006		0.007 ± 0.008	1.500 ± 0.231	1.020 ± 0.171		0.056 ± 0.010	0.005 ± 0.004	0.038 ± 0.003
	w	1.2×10^4	0.042 ± 0.009	0.021 ± 0.020	0.013 ± 0.001	1.3×10^4	0.037 ± 0.007	0.000 ± 0.000	0.038 ± 0.002	6.4×10^5	0.046 ± 0.024	0.028 ± 0.019	0.025 ± 0.004
	w/o		0.209 ± 0.015	0.019 ± 0.002	0.092 ± 0.006		0.351 ± 0.027	0.016 ± 0.003	0.149 ± 0.007		0.018 ± 0.005	0.010 ± 0.011	0.018 ± 0.003
	w	1.8×10^5	0.083 ± 0.005	0.026 ± 0.004	0.021 ± 0.002	1.8×10^5	0.024 ± 0.002	0.003 ± 0.003	0.021 ± 0.0008	5.9×10^6	0.049 ± 0.006	0.015 ± 0.004	0.022 ± 0.001
	w/o		0.037 ± 0.005	0.016 ± 0.007	0.017 ± 0.002		0.077 ± 0.007	0.004 ± 0.003	0.060 ± 0.004		0.042 ± 0.009	0.017 ± 0.007	0.021 ± 0.002
	w	1.6×10^6	0.066 ± 0.005	0.032 ± 0.007	0.009 ± 0.001	2.5×10^6	0.046 ± 0.0002	0.001 ± 0.003	0.045 ± 0.001				
	w/o		0.038 ± 0.005	0.016 ± 0.007	0.015 ± 0.001		0.063 ± 0.005	0.032 ± 0.008	0.012 ± 0.001				
	w	2.7×10^7	0.020 ± 0.003	0.032 ± 0.012	0.003 ± 0.0006	3.6×10^6	0.051 ± 0.005	0.006 ± 0.004	0.042 ± 0.002				
	w/o		0.244 ± 0.030	0.025 ± 0.009	0.063 ± 0.006		0.011 ± 0.002	0.009 ± 0.004	0.022 ± 0.002				
MQS	w	8.7×10^3	0.093 ± 0.005	0.019 ± 0.001	0.028 ± 0.003	3.9×10^4	0.070 ± 0.006	0.011 ± 0.003	0.036 ± 0.002	8.9×10^3	0.136 ± 0.013	0.004 ± 0.003	0.114 ± 0.004
	w/o		0.064 ± 0.009	0.017 ± 0.004	0.029 ± 0.003		0.094 ± 0.005	0.002 ± 0.002	0.083 ± 0.001		0.117 ± 0.006	0.008 ± 0.002	0.078 ± 0.002
	w	1.2×10^4	0.258 ± 0.016	0.031 ± 0.006	0.049 ± 0.007	3.7×10^4	0.126 ± 0.009	0.010 ± 0.003	0.074 ± 0.003	1.1×10^5	0.162 ± 0.017	0.009 ± 0.004	0.103 ± 0.003
	w/o		0.199 ± 0.019	0.029 ± 0.007	0.038 ± 0.005		0.175 ± 0.012	0.018 ± 0.003	0.084 ± 0.005		0.124 ± 0.014	0.008 ± 0.004	0.090 ± 0.005
	w	1.1×10^5	0.095 ± 0.008	0.023 ± 0.005	0.028 ± 0.001	1.9×10^5	0.340 ± 0.031	0.044 ± 0.012	0.079 ± 0.005	1.6×10^6	0.303 ± 0.037	0.012 ± 0.006	0.171 ± 0.013
	w/o		0.058 ± 0.002	0.015 ± 0.001	0.026 ± 0.001		0.135 ± 0.008	0.019 ± 0.003	0.067 ± 0.005		0.123 ± 0.010	0.013 ± 0.003	0.062 ± 0.005
	w	1.9×10^5	0.079 ± 0.012	0.009 ± 0.004	0.045 ± 0.003	3.0×10^5	0.083 ± 0.003	0.008 ± 0.001	0.051 ± 0.002	5.6×10^6	0.152 ± 0.0122	0.033 ± 0.009	0.025 ± 0.004
	w/o		0.061 ± 0.007	0.010 ± 0.004	0.036 ± 0.002		0.238 ± 0.014	0.022 ± 0.005	0.069 ± 0.007		0.029 ± 0.006	0.012 ± 0.009	0.015 ± 0.001
	w	2.1×10^7	0.154 ± 0.023	0.028 ± 0.010	0.037 ± 0.003	2.4×10^7	0.154 ± 0.019	0.017 ± 0.006	0.066 ± 0.003				
	w/o		0.131 ± 0.026	0.032 ± 0.014	0.024 ± 0.003		0.224 ± 0.042	0.024 ± 0.014	0.068 ± 0.004				
CQS	w	0.9×10^3	0.058 ± 0.013	0.034 ± 0.024	0.010 ± 0.002	0.2×10^3	0.101 ± 0.018	0.007 ± 0.013	0.134 ± 0.012	8.5×10^4	0.035 ± 0.018	0.030 ± 0.028	0.010 ± 0.003
	w/o		0.528 ± 0.104	0.021 ± 0.015	0.390 ± 0.059		1.760 ± 0.733	0.056 ± 0.155	1.460 ± 0.170		0.016 ± 0.021	0.015 ± 0.006	0.075 ± 0.005
	w	3.4×10^3	0.018 ± 0.005	0.035 ± 0.008	0.074 ± 0.009	4.2×10^3	0.071 ± 0.005	0.001 ± 0.002	0.065 ± 0.004	5.8×10^5	0.068 ± 0.017	0.046 ± 0.028	0.015 ± 0.003
	w/o		0.018 ± 0.005	0.035 ± 0.008	0.074 ± 0.009		0.679 ± 0.048	0.037 ± 0.007	0.197 ± 0.017		0.053 ± 0.039	0.036 ± 0.091	0.021 ± 0.007
	w	1×10^5	0.020 ± 0.003	0.025 ± 0.009	0.005 ± 0.001	6.8×10^4	0.048 ± 0.010	0.000 ± 0.000	0.062 ± 0.005	6.6×10^6	0.208 ± 0.019	0.058 ± 0.013	0.018 ± 0.005
	w/o		0.033 ± 0.003	0.007 ± 0.003	0.022 ± 0.001		0.145 ± 0.029	0.005 ± 0.006	0.103 ± 0.008		0.067 ± 0.034	0.059 ± 0.043	0.007 ± 0.0009
	w	1.2×10^6	0.132 ± 0.016	0.042 ± 0.009	0.014 ± 0.003	6.6×10^5	0.049 ± 0.009	0.001 ± 0.005	0.052 ± 0.006				
	w/o		0.130 ± 0.016	0.039 ± 0.009	0.016 ± 0.007		0.032 ± 0.009	0.007 ± 0.010	0.026 ± 0.002				
	w	1.2×10^7	0.064 ± 0.012	0.036 ± 0.022	0.010 ± 0.002	7.3×10^7	0.080 ± 0.008	0.023 ± 0.008	0.030 ± 0.003				
	w/o		0.098 ± 0.009	0.040 ± 0.010	0.013 ± 0.001		0.073 ± 0.024	0.025 ± 0.022	0.030 ± 0.004				

[a] w – with sand and w/o – without sand.

Table 2
Fitted inactivation parameters for bacteriophage ΦX174.

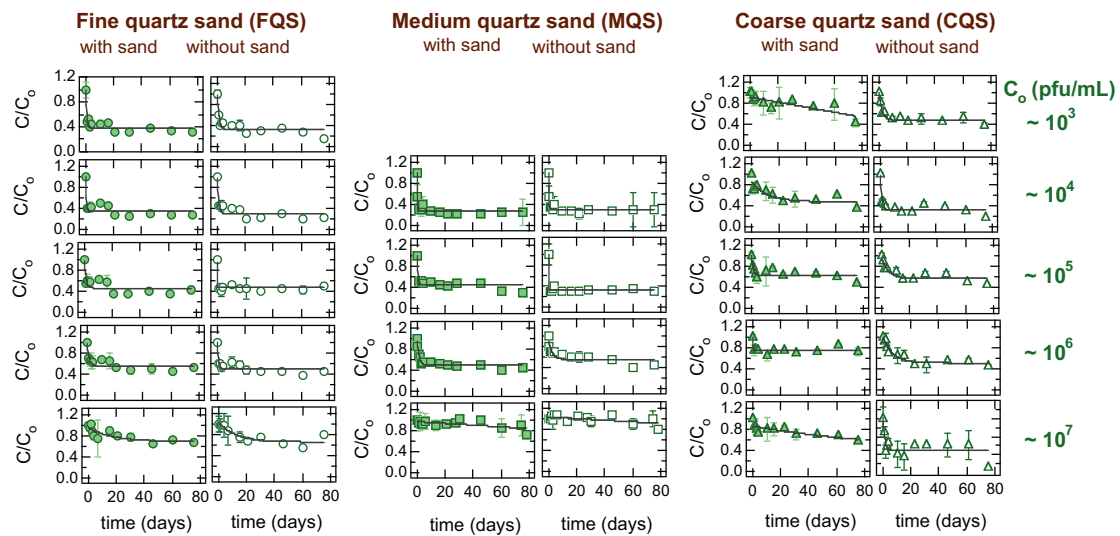| Conditions[a]		Static batch experiments at 4 °C				Static batch experiments at 20 °C				Dynamic batch experiments at 4 °C			
		C_0 (pfu/mL)	λ_0 (day^{-1})	α (day^{-1})	λ (day^{-1})	C_0 (pfu/mL)	λ_0 (day^{-1})	α (day^{-1})	λ (day^{-1})	C_0 (pfu/mL)	λ_0 (day^{-1})	α (day^{-1})	λ (day^{-1})
FQS	w	5.6×10^3	0.234 ± 0.047	0.044 ± 0.020	0.022 ± 0.005	3.3×10^3	0.038 ± 0.004	0.002 ± 0.002	0.035 ± 0.008	1.06×10^5	0.050 ± 0.005	0.003 ± 0.003	0.028 ± 0.002
	w/o		0.227 ± 0.039	0.039 ± 0.017	0.027 ± 0.049		0.042 ± 0.010	0.001 ± 0.006	0.045 ± 0.002		0.018 ± 0.009	0.013 ± 0.005	0.032 ± 0.002
	w	6.5×10^4	0.256 ± 0.021	0.044 ± 0.014	0.025 ± 0.006	3.4×10^4	0.084 ± 0.013	0.021 ± 0.008	0.028 ± 0.002	1.4×10^6	0.017 ± 0.005	0.012 ± 0.004	0.029 ± 0.004
	w/o		0.263 ± 0.041	0.041 ± 0.016	0.028 ± 0.006		0.029 ± 0.003	0.004 ± 0.003	0.040 ± 0.002		0.022 ± 0.008	0.011 ± 0.007	0.024 ± 0.001
	w	5×10^5	0.167 ± 0.036	0.041 ± 0.023	0.018 ± 0.004	3.4×10^5	0.024 ± 0.004	0.004 ± 0.004	0.020 ± 0.0009	2.3×10^7	0.009 ± 0.006	0.036 ± 0.005	0.063 ± 0.004
	w/o		0.234 ± 0.032	0.050 ± 0.003	0.016 ± 0.005		0.018 ± 0.003	0.001 ± 0.001	0.019 ± 0.001		0.015 ± 0.0004	0.003 ± 0.0008	0.019 ± 0.001
	w	1.8×10^6	0.038 ± 0.008	0.033 ± 0.013	0.007 ± 0.001	5×10^6	0.078 ± 0.006	0.023 ± 0.006	0.023 ± 0.002				
	w/o		0.014 ± 0.003	0.012 ± 0.08	0.008 ± 0.001		0.018 ± 0.002	0.004 ± 0.004	0.016 ± 0.0007				
	w	9×10^6	0.125 ± 0.013	0.041 ± 0.015	0.014 ± 0.003	1.5×10^8	0.063 ± 0.007	0.023 ± 0.009	0.018 ± 0.002				
	w/o		0.165 ± 0.016	0.043 ± 0.016	0.016 ± 0.003		0.028 ± 0.004	0.005 ± 0.005	0.022 ± 0.001				
MQS	w	4.5×10^3	0.048 ± 0.006	0.024 ± 0.009	0.012 ± 0.001	7.5×10^3	0.577 ± 0.005	0.014 ± 0.003	0.026 ± 0.002	4.2×10^3	0.012 ± 0.002	0.005 ± 0.003	0.010 ± 0.0009
	w/o		0.023 ± 0.005	0.015 ± 0.008	0.010 ± 0.0009		0.168 ± 0.014	0.023 ± 0.006	0.050 ± 0.003		0.045 ± 0.006	0.020 ± 0.009	0.016 ± 0.001
	w	6.9×10^4	0.496 ± 0.023	0.055 ± 0.008	0.029 ± 0.008	9×10^4	0.213 ± 0.021	0.047 ± 0.016	0.018 ± 0.004	5.7×10^4	0.044 ± 0.004	0.024 ± 0.007	0.012 ± 0.001
	w/o		0.235 ± 0.022	0.055 ± 0.008	0.025 ± 0.007		0.106 ± 0.009	0.032 ± 0.008	0.020 ± 0.002		0.006 ± 0.001	0.007 ± 0.006	0.005 ± 0.0005
	w	5.9×10^5	0.010 ± 0.004	0.021 ± 0.030	0.003 ± 0.0004	5.5×10^4	0.134 ± 0.014	0.012 ± 0.004	0.065 ± 0.008	9.2×10^4	0.001 ± 0.003	0.040 ± 0.014	0.009 ± 0.0009
	w/o		0.007 ± 0.0007	0.040 ± 0.008	0.002 ± 0.0002		0.421 ± 0.004	0.038 ± 0.006	0.054 ± 0.010		0.047 ± 0.008	0.031 ± 0.062	0.010 ± 0.001
	w	7.1×10^7	0.200 ± 0.001	0.044 ± 0.008	0.020 ± 0.004	5.5×10^5	0.059 ± 0.006	0.015 ± 0.004	0.026 ± 0.003	1.5×10^6	0.053 ± 0.005	0.044 ± 0.003	0.006 ± 0.0005
	w/o		0.317 ± 0.025	0.047 ± 0.009	0.023 ± 0.007		0.039 ± 0.006	0.011 ± 0.005	0.021 ± 0.003		0.031 ± 0.003	0.036 ± 0.009	0.005 ± 0.0006
	w	3.6×10^7	0.188 ± 0.027	0.047 ± 0.007	0.016 ± 0.003	6.3×10^5	0.080 ± 0.007	0.021 ± 0.002	0.024 ± 0.004	5.8×10^6	0.075 ± 0.003	0.039 ± 0.004	0.008 ± 0.001
	w/o		0.148 ± 0.017	0.045 ± 0.007	0.014 ± 0.002		0.085 ± 0.012	0.014 ± 0.006	0.038 ± 0.004		0.099 ± 0.014	0.055 ± 0.026	0.004 ± 0.002
CQS	w	1.7×10^3	0.028 ± 0.009	0.025 ± 0.014	0.008 ± 0.001	1.7×10^3	0.126 ± 0.011	0.029 ± 0.005	0.025 ± 0.003	2×10^4	0.050 ± 0.005	0.046 ± 0.012	0.004 ± 0.001
	w/o		0.136 ± 0.014	0.040 ± 0.009	0.016 ± 0.003		0.280 ± 0.016	0.027 ± 0.004	0.065 ± 0.005		0.145 ± 0.022	0.047 ± 0.071	0.013 ± 0.003
	w	2.5×10^4	0.103 ± 0.012	0.037 ± 0.013	0.015 ± 0.002	2.5×10^4	0.235 ± 0.042	0.043 ± 0.025	0.025 ± 0.006	1.7×10^5	0.057 ± 0.005	0.040 ± 0.009	0.007 ± 0.007
	w/o		0.261 ± 0.014	0.044 ± 0.007	0.026 ± 0.006		0.359 ± 0.034	0.029 ± 0.007	0.076 ± 0.008		0.061 ± 0.014	0.034 ± 0.018	0.010 ± 0.002
	w	1.5×10^5	0.100 ± 0.008	0.042 ± 0.013	0.011 ± 0.002	1.5×10^5	0.133 ± 0.012	0.035 ± 0.007	0.021 ± 0.003	2×10^6	0.063 ± 0.016	0.038 ± 0.012	0.010 ± 0.003
	w/o		0.079 ± 0.011	0.035 ± 0.011	0.012 ± 0.002		0.252 ± 0.030	0.034 ± 0.015	0.042 ± 0.005		0.035 ± 0.005	0.017 ± 0.005	0.014 ± 0.001
	w	2×10^6	0.091 ± 0.004	0.053 ± 0.007	0.006 ± 0.002	2×10^6	0.275 ± 0.003	0.042 ± 0.017	0.032 ± 0.008				
	w/o		0.059 ± 0.003	0.028 ± 0.003	0.013 ± 0.002		0.196 ± 0.027	0.028 ± 0.012	0.044 ± 0.004				
	w	2×10^7	0.058 ± 0.005	0.039 ± 0.014	0.008 ± 0.001	2×10^7	0.159 ± 0.012	0.035 ± 0.004	0.024 ± 0.006				
	w/o		0.098 ± 0.009	0.044 ± 0.009	0.010 ± 0.002		0.191 ± 0.010	0.028 ± 0.006	0.042 ± 0.004				

[a] w – with sand and w/o – without sand.

Fig. 3. Experimental data for ΦX174 inactivation under static batch conditions with sand (solid symbols) and without sand (open symbols) at 4 °C, and simulated concentration histories (solid curves). The first row of graphs corresponds to virus initial concentration of $C_0 = 10^3$ pfu/mL, the second, third, fourth and fifth rows to $C_0 = 10^4$, 10^5, 10^6, and 10^7 pfu/mL, respectively. The circles, squares, and triangles represent experiments with FQS, MQS, and CQS, respectively. Error bars not shown are smaller than the size of the symbol.

CQS), the inactivation of both MS2 and ΦX174 under static conditions at 4 °C is generally faster without the presence of sand. Comparison of the batch inactivation data of MS2 and ΦX174 at 4 °C suggests that the inactivation rate of MS2 is greater than that of ΦX174. Also, the experimental data suggested that the inactivation rates for both MS2 and ΦX174, with and without the presence of sand, decrease with increasing initial virus concentration. Furthermore, no significant differences in the inactivation rates were observed between the three different sizes of quartz sand (FQS, MQS, and CQS) employed in this study. Consequently, no obvious relationship between the quartz sand particle size and virus inactivation could be established.

The experimental data from the batch experiments of MS2 and ΦX174 inactivation at 20 °C together with the simulated concentrations based on the time-dependent inactivation model are shown in Figs. 4 and 5, respectively. Also, the fitted inactivation parameter values (λ_0, α and λ) for MS2 are listed in Table 1, and for ΦX174 are

listed in Table 2. Over all the experimental results at 20 °C follow very similar trends as those observed for the experiments at 4 °C. However, comparison of the parameter values in Tables 1 and 2 suggest that inactivation is affected by the ambient temperature. In general, the resistivity to virus inactivation, α, is greater at 4 °C than 20 °C. Furthermore, the inactivation coefficient, λ, is greater at 20 °C than 4 °C. Therefore, in agreement with previous studies, the inactivation rate of both MS2 and ΦX174 increases with temperature [45,56]. Clearly, the batch inactivation data of MS2 and ΦX174 at 20 °C suggest that the inactivation rate of MS2 is greater than that of ΦX174.

Figs. 6 and 7 show the bacteriophages inactivation experimental data from the dynamic batch experiment at 4 °C with and without sand, together with the corresponding simulated concentrations for time-dependent inactivation rate. Tables 1 and 2 present the fitted inactivation parameters for MS2 and ΦX174, respectively. The experimental data indicate that virus inactivation under dynamic
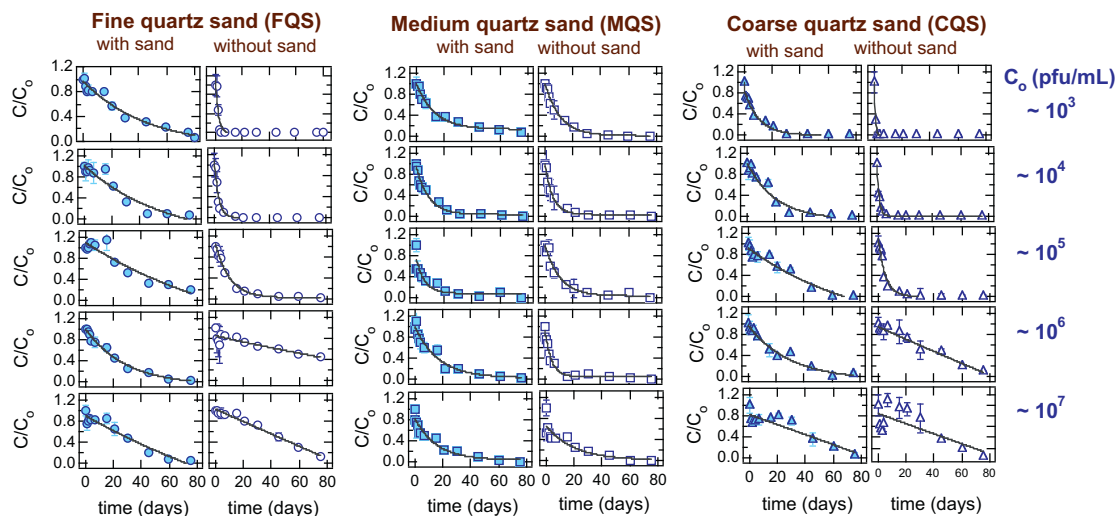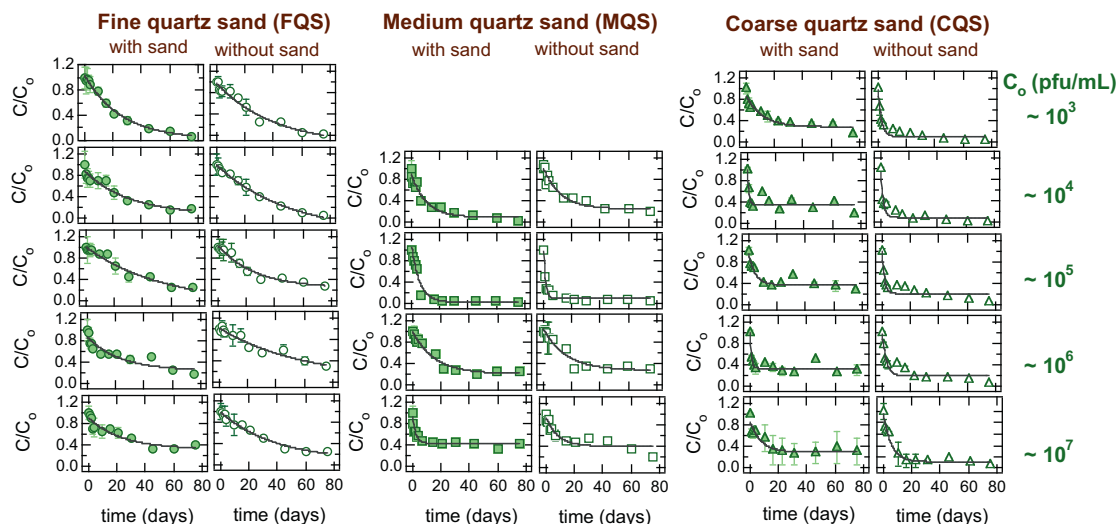

Fig. 4. Experimental data for MS2 inactivation under static batch conditions with sand (solid symbols) and without sand (open symbols) at 20 °C, and simulated concentration histories (solid curves). The first row of graphs corresponds to virus initial concentration of $C_0 = 10^3$ pfu/mL, the second, third, forth and fifth rows to $C_0 = 10^4$, 10^5, 10^6, and 10^7 pfu/mL, respectively. The circles, squares, and triangles represent experiments with FQS, MQS, and CQS, respectively. Error bars not shown are smaller than the size of the symbol.
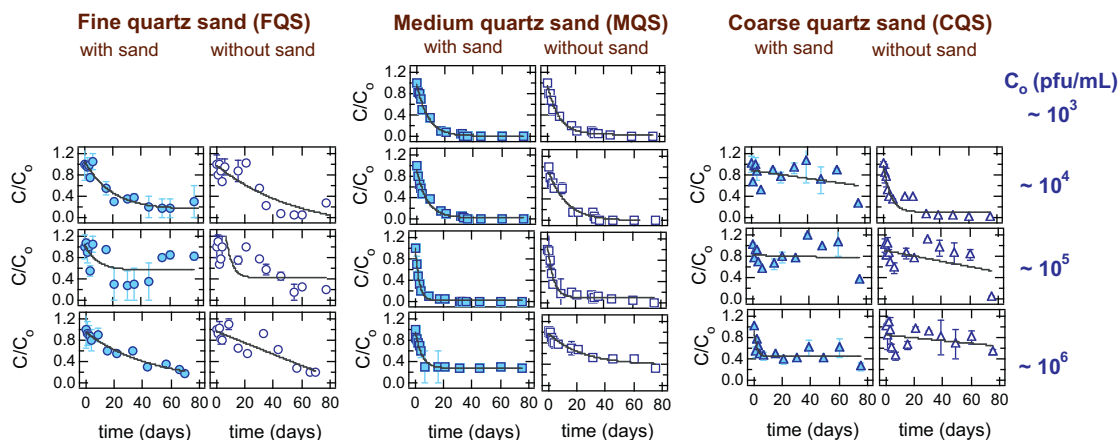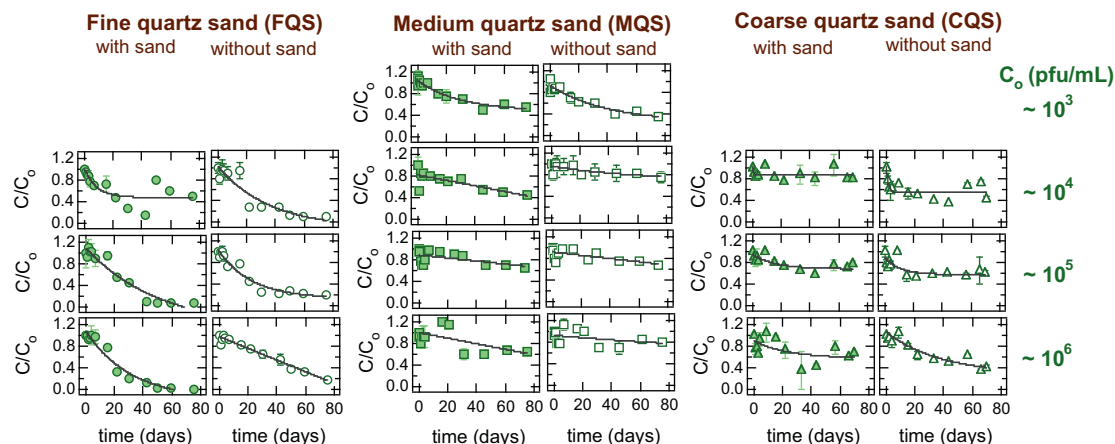
Fig. 5. Experimental data for ΦX174 inactivation under static batch conditions with sand (solid symbols) and without sand (open symbols) at 20 °C, and simulated concentration histories (solid curves). The first row of graphs corresponds to virus initial concentration of $C_0 = 10^3$ pfu/mL, the second, third, fourth and fifth rows to $C_0 = 10^4$, 10^5, 10^6, and 10^7 pfu/mL, respectively. The circles, squares, and triangles represent experiments with FQS, MQS, and CQS, respectively. Error bars not shown are smaller than the size of the symbol.
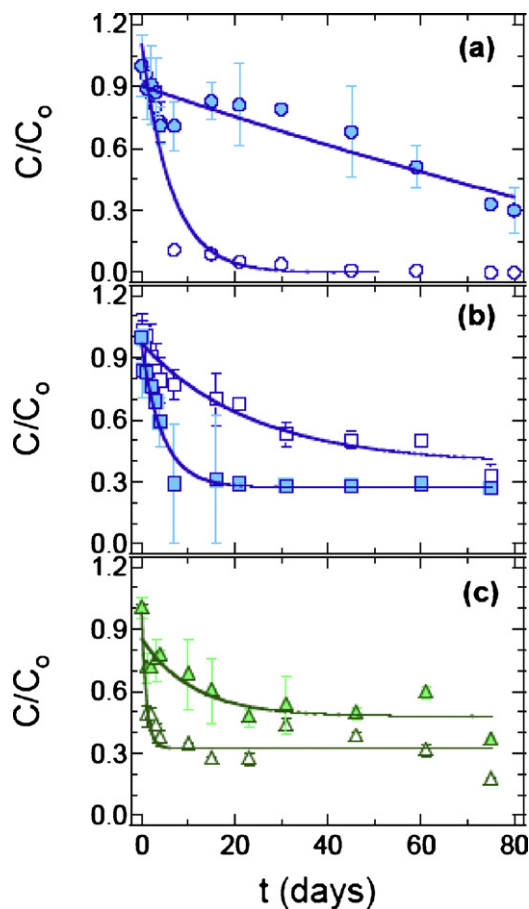

Fig. 6. Experimental data for MS2 inactivation under dynamic batch conditions with sand (solid symbols) and without sand (open symbols) at 4 °C, and simulated concentration histories (solid curves). The first row of graphs corresponds to virus initial concentration of $C_0 = 10^3$ pfu/mL, the second, third, and fourth rows to $C_0 = 10^4$, 10^5, and 10^6 pfu/mL, respectively. The circles, squares, and triangles represent experiments with FQS, MQS, and CQS, respectively. Error bars not shown are smaller than the size of the symbol.

Fig. 7. Experimental data for ΦX174 inactivation under dynamic batch conditions with sand (solid symbols) and without sand (open symbols) at 4 °C, and simulated concentration histories (solid curves). The first row of graphs corresponds to virus initial concentration of $C_0 = 10^3$ pfu/mL, the second, third, and fourth rows to $C_0 = 10^4$, 10^5, and 10^6 pfu/mL, respectively. The circles, squares, and triangles represent experiments with FQS, MQS, and CQS, respectively. Error bars not shown are smaller than the size of the symbol.

Fig. 8. Comparison between selective virus inactivation experimental data in the presence (solid symbols), and absence of sand (open symbols) for: (a) MS2 with FQS under static batch conditions, (b) MS2 with MQS under dynamic batch conditions, and (c) ΦX174 with CQS under static batch conditions. The solid curves correspond to simulated concentration histories. Here $C_0 = \sim 10^4$ pfu/mL at 4 °C. Error bars not shown are smaller than the size of the symbol.

Fig. 9. Comparison between selective MS2 (open circles), and ΦX174 (crossed circles) inactivation experimental data under static conditions in the absence of sand at: (a) 4 °C, and (b) 20 °C. The solid curves correspond to simulated concentration histories. Here $C_0 = \sim 10^4$ pfu/mL. Error bars not shown are smaller than the size of the symbol.

conditions is slightly higher than static conditions, especially in the presence of the sands because agitation improves the contact of particles with the liquid and decreases the resistance to mass transfer [49]. Furthermore, in agreement with the batch static experiments, the data from the dynamic experiments suggest that the inactivation rate of MS2 is greater than that of ΦX174. Worthy to note is that, contrary to the static batch experiments, MS2 and ΦX174 inactivation under dynamic conditions is generally faster in the presence of sand, suggesting that moving sand grains do not offer protection against virus inactivation.

To better illustrate the main results of this study, selective experimental data are compared. Fig. 8 shows that the presence of sand protects viruses from inactivation under static conditions (Fig. 8a and c) but not under dynamic conditions (Fig. 8b). Fig. 9 illustrates that MS2 inactivation is faster than that of ΦX174, and that virus inactivation is greater at higher temperatures. Fig. 10 shows that virus inactivation decreases with increasing initial virus concentration. Finally, Fig. 11 illustrates graphically the variability of the various inactivation rate coefficients estimated in this study.

5. Discussion

The experimental results from the batch experiments of MS2 and ΦX174 inactivation showed that the simulated concentrations for the time-dependent inactivation match the experimental data much better than using constant inactivation rates. Similar
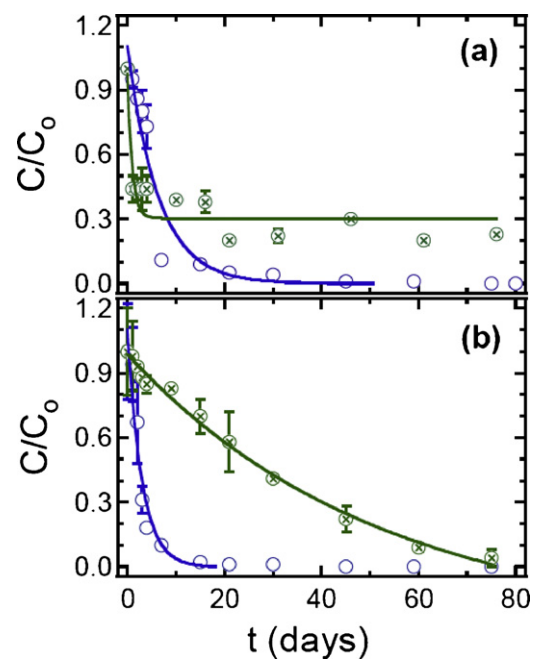
observations have also been reported in the literature by other investigators [42,45]. Worthy to note is that the temporal variability of the inactivation rate coefficient is often attributed to multiphasic sequential inactivation, which is caused by the presence of two or more subpopulations (e.g. different aggregate sizes) of bacteriophages that may exhibit different sensitivity to temperature [37,41,44]. Therefore, the most sensitive subpopulations undergo
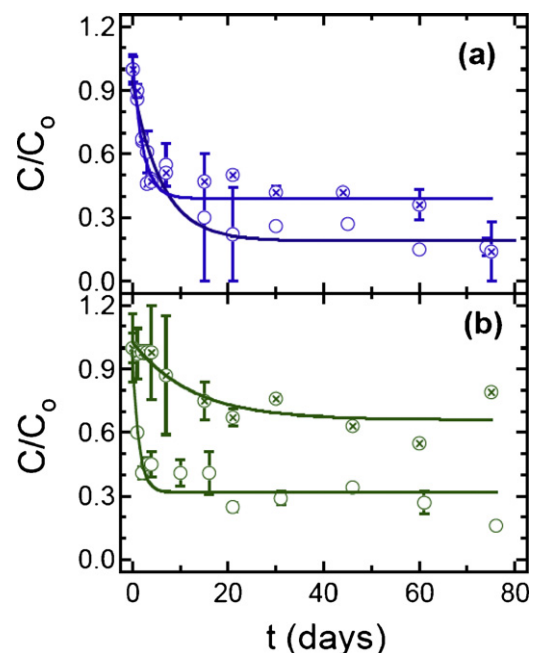

Fig. 10. Comparison between selective virus inactivation experimental data at 4 °C with initial concentration $C_0 = \sim 10^3$ pfu/mL (open circles) and $C_0 = \sim 10^7$ pfu/mL (crossed circles) under static conditions in the absence of sand for: (a) MS2, and (b) ΦX174. The solid curves correspond to simulated concentration histories. Error bars not shown are smaller than the size of the symbol.
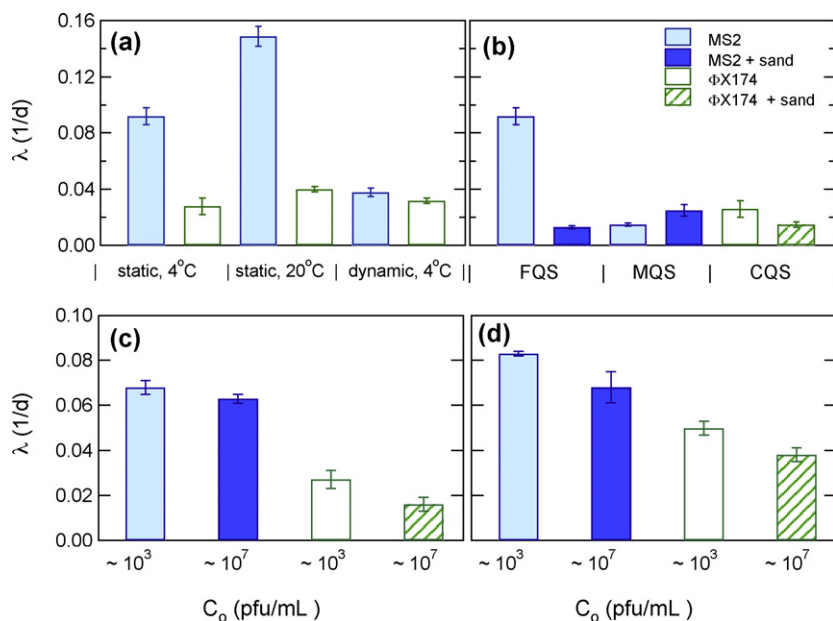
Fig. 11. Comparison between selective virus inactivation rates under different conditions: (a) initial concentration $C_0 = \sim 10^4$ pfu/mL, (b) static conditions with FQS and dynamic conditions with MSQ at 4 °C and initial concentration $C_0 = \sim 10^4$ pfu/mL, (c) static conditions at 4 °C, and (d) static conditions at 20 °C.

rapid inactivation and the more resistive subpopulations undergo slower inactivation. However, the overall inactivation is controlled by the dominant subpopulation [42].

In this study observed that the inactivation of both MS2 and ΦX174 under static conditions at 4 °C is generally faster without the presence of sand. This leads to the conclusion that the attachment of viruses on quartz sand grains can offer protection against virus inactivation. This result is in agreement with many previous studies [14,38,40,52–54]. Moreover, the results for both of the viruses examined, MS2 and ΦX174, showed that the virus inactivation rates decrease with increasing initial virus concentration. This is attributed to possible increased virus aggregation with increased initial virus concentration. Virus aggregation is known to reduce significantly the inactivation rate [55].

The experimental results, under dynamic conditions showed that in the presence of the sands, the virus inactivation rates were increased compared to the virus inactivation rates under static conditions. This increase in inactivation is attributed to the presence of air–liquid and air–solid interfaces. This result is consistent with previous studies reported in the literature [45,50,57]. Note that dynamic conditions lead to breakage of virus aggregates and to a continuous virus attachment onto, and detachment from moving quartz sand grains. Furthermore, it is worthy to mention that the hydrophobic protein coat of MS2 may contribute to the observed enhanced attachment of MS2 onto quartz sand grains, as well as to possible attraction to the air–water interface. Also, the hydrophilic protein coat of ΦX174 may not be strongly attracted to the air–water interface. Consequently, MS2 inactivation rates under dynamic conditions would be greater than ΦX174 inactivation rates.

6. Conclusions

The experimental results of this work indicate that temperature plays a significant role in virus inactivation. Both MS2 and ΦX174 remain infective for longer periods of time at low temperatures (4 °C) than at high temperatures (20 °C). The attachment of viruses onto solid surfaces affects virus inactivation. It was observed that under static batch conditions the attachment of

viruses onto solid surfaces offers a protection against inactivation. However, no obvious relationship between quartz sand particle size and virus inactivation could be established from the experimental data. The initial virus concentration can significantly affect virus inactivation. Low initial virus concentrations yielded higher inactivation rates, compared to high initial virus concentrations. Furthermore, the inactivation rate of MS2 was shown to be greater than that of ΦX174.

Acknowledgments

References

[1] WHO, Guidelines for the safe use of wastewater, excreta and greywater, World Health Organization, Geneva, Switzerland, 2006.
[2] M. Abbaszadegan, M. Lechevallier, C.P. Gerba, Occurrence of viruses in US ground waters, J. Am. Water Works Assoc. 95 (2003) 107–120.
[3] G.F. Craun, M.F. Craun, R.L. Calderon, M.J. Beach, Waterborne outbreaks reported in the United States, J. Water Health 4 (2006) 19–30.
[4] F.M. Wellings, A.L. Lewis, C.W. Mountain, L.V. Pierce, Demonstration of virus in groundwater after effluent discharge onto soil, Appl. Microbiol. 29 (1975) 751–757.
[5] J.P. Loveland, J.N. Ryan, G.L. Amy, R.W. Harvey, The reversibility of virus attachment to mineral surfaces, Colloids Surf. A: Physicochem. Eng. Aspects 107 (1996) 205–221.
[6] J.N. Ryan, R.W. Harvey, D. Metge, M. Elimelech, T. Navigato, A.P. Pieper, Field and laboratory investigations of inactivation of viruses (PRD1 and MS2) attached to iron oxide-coated quartz sand, Environ. Sci. Technol. 36 (2002) 2403–2413.
[7] R. Anders, C.V. Chrysikopoulos, Virus fate and transport during artificial recharge with recycled water, Water Resour. Res. 41 (2005) W10415, http://dx.doi.org/10.1029/2004WR003419.
[8] M.V. Yates, C.P. Gerba, L.M. Kelly, Virus persistence in groundwater, Appl. Environ. Microbiol. 49 (1985) 778–781.

[9] C.V. Chrysikopoulos, Y. Sim, One-dimensional virus transport in homogeneous porous media with time-dependent distribution coefficient, J. Hydrol. 185 (1996) 199–219.

[10] R.J. Hunt, M.A. Borchard, K.D. Richards, S.K. Spencer, Assessment of sewer source contamination of drinking water wells using tracers and human enteric viruses, Environ. Sci. Technol. 44 (2010) 7956–7963.

[11] R. Maxwell, C. Welty, A. Tompson, Streamline-based simulation of virus transport resulting from long term artificial research in a heterogeneous aquifer, Adv. Water Resour. 22 (2003) 203–221.

[12] C. Masciopinto, R. La Mantia, C.V. Chrysikopoulos, Fate and transport of pathogens in a fractured aquifer in the Salento area, Italy, Water Resour. Res. 44 (2008) W01404, http://dx.doi.org/10.1029/2006WR005643.

[13] B.H. Keswick, C.P. Gerba, Viruses in groundwater, Environ. Sci. Technol. 14 (1980) 1290–1297.

[14] C.P. Gerba, Applied and theoretical aspects of virus adsorption to surfaces, Adv. Appl. Microbiol. 30 (1984) 133–168.

[15] M.V. Yates, S.R. Yates, J. Wagner, C.P. Gerba, Modelling virus survival and transport in the subsurface, J. Contam. Hydrol. 1 (1987) 329–345.

[16] Y. Sim, C.V. Chrysikopoulos, Analytical models for one-dimensional virus transport in saturated porous media, Water. Resour. Res. 31 (1995) 1429–1437 (Correction, Water Resour. Res. 32 (1996) 1473).

[17] Y. Jin, M.V. Yates, S.S. Thompson, W.A. Jury, Sorption of viruses during flow through saturated sand columns, Environ. Sci. Technol. 31 (1997) 548–555.

[18] Y. Sim, C.V. Chrysikopoulos, Three-dimensional analytical models for virus transport in saturated porous media, Transp. Porous Media 30 (1998) 87–112.

[19] Y. Sim, C.V. Chrysikopoulos, Analytical solutions for solute transport in saturated porous media with semi-infinite or finite thickness, Adv. Water Resour. 22 (1999) 507–519.

[20] Y. Sim, C.V. Chrysikopoulos, Virus transport in unsaturated porous media, Water Resour. Res. 36 (2000) 173–179.

[21] R.W. Harvey, J.N. Ryan, Use of PRD1 bacteriophage in groundwater viral transport, inactivation, and attachment studies, FEMS Microbiol. Ecol. 49 (2004) 3–16.

[22] D.E. John, J.B. Rose, Review of factors affecting microbial survival in groundwater, Environ. Sci. Technol. 39 (2005) 7345–7356.

[23] R. Anders, C.V. Chrysikopoulos, Transport of viruses through saturated and unsaturated columns packed with sand, Transp. Porous Media 76 (2009) 121–138.

[24] C.V. Chrysikopoulos, C. Masciopinto, R. La Mantia, I.D. Manariotis, Removal of biocolloids suspended in reclaimed wastewater by injection in a fractured aquifer model, Environ. Sci. Technol. 44 (2010) 971–977.

[25] T.K. Sen, Processes in pathogenic biocolloidal contaminants transport in saturated and unsaturated porous media: a review, Water Air Soil Pollut. 216 (2011) 239–256.

[26] J. Zhuang, Y. Jin, Virus retention and transport through Al-oxide coated sand columns: effects of ionic strength and composition, J. Contam. Hydrol. 60 (2003) 193–209.

[27] N. Tufenkji, Modeling microbial transport in porous media: Traditional approaches and recent developments, Adv. Water Resour. 30 (2007) 1455–1469.

[28] V.I. Syngouna, C.V. Chrysikopoulos, Transport of biocolloids in water saturated columns packed with sand: effect of grain size and pore water velocity, J. Contam. Hydrol. 126 (2011) 301–314.

[29] R. Attinti, H. Wei, K. Kniel, J.T. Sims, Y. Jin, Virus' (MS2, X174, and Aichi) attachment on sand measured by atomic force microscopy and their transport through sand columns, Environ. Sci. Technol. 44 (2010) 2426–2432.

[30] C.V. Chrysikopoulos, V.I. Syngouna, Attachment of bacteriophages MS2 and ΦX174 onto kaolinite and montmorillonite: extended-DLVO interactions, Colloids Surf. B: Biointerfaces 92 (2012) 74–83.

[31] B.L. Yuan, M. Pham, T.H. Nguyen, Deposition kinetics of bacteriophage MS2 on a silica surface coated with natural organic matter in a radial stagnation point flow cell, Environ. Sci. Technol. 42 (2008) 7628–7633.

[32] G.E. Walshe, L. Pang, M. Flury, M.E. Close, M. Flintoft, Effects of pH, ionic strength, dissolved organic matter, and flow rate on the cotransport of MS2 bacteriophages with kaolinite in gravel aquifer media, Water Res. 44 (2010) 1255–1269.

[33] J. Zhuang, Y. Jin, Virus retention and transport through as influenced by different forms of soil organic matter, J. Environ. Qual. 32 (2003) 816–883.

[34] A.A. Keller, S. Sirivithayapakorn, C.V. Chrysikopoulos, Early breakthrough of colloids and bacteriophage MS2 in a water-saturated sand column, Water Resour. Res. 40 (2004) W08304, http://dx.doi.org/10.1029/2003WR002676.

[35] S. Van Cuyk, R.L. Siegrist, Virus removal within a soil infiltration zone as affected by effluent composition, application rate, and soil type, Water Res. 41 (2007) 699–709.

[36] L. Cheng, A.S. Chetochine, I.L. Pepper, M.L. Brusseau, Influence of DOC on MS-2 bacteriophage transport in a sandy soil, Water Air Soil Pollut. 178 (2007) 315–322.

[37] C.J. Hurst, C.P. Gerba, I. Cech, Effects of environmental variables and soil characteristics on virus survival in soil, Appl. Environ. Microbiol. 40 (1980) 1067–1079.

[38] M.D. Sobsey, C.H. Dean, M.E. Knuckles, R.A. Wagner, Interactions and survival of enteric viruses in soil materials, Appl. Environ. Microbiol. 40 (1980) 92–101.

[39] J. Jansons, L.W. Edmonds, B. Speight, M.R. Bucens, Survival of viruses in groundwater, Water Res. 23 (1989) 301–306.

[40] S.B. Grant, E.J. List, M.E. Lidstrom, Kinetic analysis of virus adsorption and inactivation in batch experiments, Water Resour. Res. 29 (1993) 2067–2085.

[41] S.B. Grant, Inactivation kinetics of viral aggregates, J. Environ. Eng. 121 (1995) 311–319.

[42] Y. Sim, C.V. Chrysikopoulos, One-dimensional virus transport in porous media with time dependent inactivation rate coefficients, Water Resour. Res. 32 (1996) 2607–2611.

[43] Y. Sim, C.V. Chrysikopoulos, Analytical models for virus adsorption and inactivation in unsaturated porous media, Colloids Surf. A: Physicochem. Eng. Aspects 155 (1999) 189–197.

[44] C.V. Chrysikopoulos, E.T. Vogler, Estimation of time dependent virus inactivation rates by geostatistical and resampling techniques: application to virus transport in porous media, Stoch. Environ. Res. Risk Assess. 18 (2004) 67–78.

[45] R. Anders, C.V. Chrysikopoulos, Evaluation of the factors controlling the time-dependent inactivation rate coefficients of bacteriophage MS2 and PRD1, Environ. Sci. Technol. 40 (2006) 3237–3242.

[46] IAWPRC Study Group on Health Related Water Microbiology, Bacteriophages as model viruses in water quality control, Water Res. 25 (1991) 529–545.

[47] P.A. Shields, Factors influencing virus adsorption to solids, Ph.D. Dissertation, University of Florida, Gainesville, FL, 1986.

[48] M.H. Adams, Bacteriophages, Interscience, New York, 1959.

[49] V.I. Syngouna, C.V. Chrysikopoulos, Interaction between viruses and clays in static and dynamic batch systems, Environ. Sci. Technol. 44 (2010) 4539–4544.

[50] S.S. Thompson, M. Flury, M.V. Yates, W.A. Jury, Role of the air–water–solid interface in bacteriophage sorption experiments, Appl. Environ. Microbiol. 64 (1998) 304–309.

[51] L.W. Sinton, C.H. Hall, P.A. Lynch, R.J. Davies-Colley, Sunlight inactivation of fecal indicator bacteria and bacteriophages from waste stabilization pond effluent in fresh and saline water, Appl. Environ. Microbiol. 68 (2002) 3605–3613.

[52] R.C. Bales, C.P. Gerba, G.H. Grondin, S.L. Jensen, Bacteriophage transport in sandy soil and fractured tuff, Appl. Environ. Microbiol. 55 (1989) 2061–2067.

[53] R.C. Bales, S.R. Hinkle, T.W. Kroeger, K. Stocking, C.P. Gerba, Bacteriophage adsorption during transport though porous media: chemical perturbations and reversibility, Environ. Sci. Technol. 25 (1991) 2088–2095.

[54] K.E. Collins, A.A. Cronin, J. Rueedi, S. Pedley, E. Joyce, P.J. Humble, J.H. Tellam, Fate and transport of bacteriophage in UK aquifers as surrogates for pathogenic viruses, Eng. Geology 85 (2006) 33–38.

[55] M.J. Mattle, B. Crouzy, M. Brennecke, K.R. Wigginton, P. Perona, T. Kohn, Impact of virus aggregation on inactivation by peracetic acid and implications for disinfectants, Environ. Sci. Technol. 45 (2011) 7710–7717.

[56] F. Traub, S.K. Spillman, R. Wyler, Method of determining virus inactivation during sludge treatment processes, Appl. Environ. Microbiol. 52 (1986) 498–503.

[57] S. Torkzaban, S.M. Hassanizadeh, J.F. Schijven, H.H.J.L. van den Berg, Role of air–water interface on retention of viruses under unsaturated conditions, Water Resour. Res. 42 (2006) W12S14.